JOURNAL OF GUIDANCE, CONTROL, AND DYNAMICS
Vol. 34, No. 6, November–December 2011

Spin-Axis Attitude Determination and Covariances in Local Sun–Earth Frame

Jozef C. van der Ha*
Mission Design & Operations, Deming, Washington 98244

DOI: 10.2514/1.53452

This paper presents practical analytical models for spin-axis attitude determination using measurements generated by sun and Earth sensors. In particular, explicit expressions for the least-squares estimates and their associated covariance matrices are established. The adoption of the local reference frame defined by the instantaneous sun and Earth vectors leads to compact analytical results. These results provide a more immediate understanding of the attitude error covariance matrix in terms of its dependence on the sun–Earth geometry. The application of the covariance results is illustrated by using the actual geometrical in-orbit conditions of two satellites.

I. Introduction

SPIN-STABILIZATION offers an attractive and effective attitude concept for many mission applications. The gyroscopic stability provides inherent robustness to external disturbance torques and additional safe modes are not required. In particular, spin-stabilization is effective for providing pointing stability during orbit injection maneuvers by means of high-thrust solid-rocket motors or bipropellant engines. For example, geostationary satellites use this strategy for the injection into geostationary orbit from a geostationary transfer orbit [1]. Spin-stabilization has also been used for the injection of deep-space probes into their heliocentric trajectories [2].

Attitude pointing requirements during injection maneuvers are typically of the order of 0.5–1°. A pointing error in the spin-axis attitude during the injection leads to a postburn trajectory error, which needs to be corrected afterwards by thrusters using onboard propellant. Therefore, the accurate determination of the spin-axis attitude before the execution of an injection maneuver saves onboard resources and is beneficial for the satellite's lifetime [1].

Sun and Earth sensors are often used to provide two independent reference directions required by the spin-axis attitude determination algorithm. The determination of the spin-axis attitude orientation from the sensor measurements is typically performed on-ground by means of a batch least-squares (LS) estimation method. Shuster [3] published the first practical estimation techniques including the associated covariance analyses. More recently, Markley and Sedlak [4] presented a comprehensive method for spin-axis attitude determination. They use an extended Kalman filter with a seven-parameter state vector based on angular-momentum properties and illustrate its practical implementation for a few NASA missions. Further information on the attitude determination and control of spinning satellites can be found in the traditional reference book by Wertz [5] and in the author's survey paper [6].

The present paper summarizes a number of useful LS techniques for the spin-axis attitude determination on the basis of sun and Earth-sensor measurements. Results are presented for both the attitude solutions and their associated covariance matrices. Explicit expressions are given for the covariances in terms of the sensor measurement angles and their random noise specifications. The adoption of the local sun–Earth reference frame facilitates the interpretation of the covariances in terms of the geometrical conditions imposed by the Earth-sensor coverage interval, the orbital characteristics, the sun and Earth directions, and in particular the sun–Earth angle. These new results are useful for prelaunch mission analyses.

Finally, the application of the results is demonstrated using the actual geometrical orbital characteristics of the orbit injections of two satellites, i.e., NASA's CONTOUR (2002) and ESA's MSG-2 (2005). These two examples demonstrate the very different characteristics of an interplanetary trajectory injection and a geostationary orbit injection.

II. Attitude Measurement Equations

The "attitude" of a spinning satellite corresponds to the "dynamical spin-axis," which is normally defined as the unit vector along the instantaneous angular-momentum vector. For simplicity, we assume here that the angular-momentum vector always coincides with the spacecraft's body-fixed Z-axis, which is an axis of either maximum or minimum inertia. Therefore, the nutation and coning effects that are included in [4] are disregarded here.

For more detailed insights into the dynamics of the directional stability of spinning rigid and flexible satellites we refer to [7].

A. Sun-Aspect Angle

The sun-aspect angle ϑ is defined as the angle between the spin-axis direction and the sun direction represented by their unit vectors $\mathbf{Z}$ and $\mathbf{S}$, respectively, see Fig. 1:

$$\vartheta = \arccos\{\mathbf{Z} \bullet \mathbf{S}\} \tag{1}$$

The typical sun sensor for spinning satellites has a vertical and a skew slit. The measured sun angle ϑ can be obtained from the time difference between the sun's crossings over the vertical and skew slits, see for instance Wertz [5], section 7.1.1. The sun sensor also provides the spin-rate knowledge from the successive sun's crossings over the sun sensor vertical slits.

B. Earth-Aspect Angle

The typical Earth sensor for spinning satellites has two static pencil-beams which are mounted at the angles μ_i ($i = 1, 2$) with respect to the spin axis as indicated in Fig. 1, see also Wertz [5], sections 7.2.1–7.2.3. The S/E and E/S pulses refer to the instants when the pencil-beams cross the space/Earth and Earth/space boundaries. With the help of the spin-rate knowledge, the S/E and E/S pulses can readily be expressed in terms of the half-chord angles κ_i ($i = 1, 2$) as shown in Fig. 1. The κ_i angles are usually the raw measurements used in the attitude determination software.

The angle ρ shown in Fig. 1 represents the apparent Earth radius seen from the satellite. The Earth-aspect angle (which is also known as nadir angle) β represents the angle between the spin-axis $\mathbf{Z}$ and the spacecraft-to-Earth unit vector (or simply Earth vector) $\mathbf{E}$ in Fig. 1:

Received 16 December 2010; revision received 24 February 2011; accepted for publication 26 February 2011.

*Consultant; jvdha@aol.com. Senior Member AIAA.

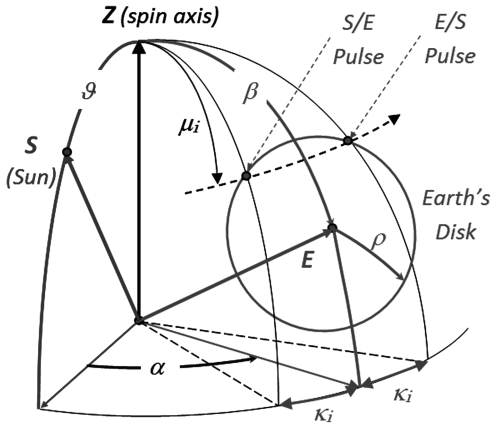

Fig. 1 Geometry of sun, Earth, spin-axis, and measurements ϑ, β, α.

$$\beta(\nu) = \arccos\{\mathbf{Z} \bullet \mathbf{E}(\nu)\} \tag{2}$$

The Earth unit vector **E** points opposite of the instantaneous orbital radius vector and rotates along with the satellite's orbital phase angle ν. Its evolution over time is determined by the orbital elements which are provided by the orbit determination.

The spherical geometry in the triangle formed by the vectors **Z**, **E**, and the S/E or E/S directions in Fig. 1 provides the following nonlinear measurement equations for the two pencil-beams $i = 1, 2$ (see, for instance, Wertz [5], Eq. 11.7):

$$\cos\mu_i \cos\beta + \sin\mu_i \sin\beta \cos\kappa_i = \cos\rho \qquad (i = 1, 2) \tag{3}$$

Equations (3) offer two implicit functional relationships for the calculation of the Earth-aspect angle β from the fundamental half-chord-angle measurements κ_i ($i = 1, 2$). This may be achieved, for instance, by using a differential correction algorithm based on a priori attitude knowledge as was done in [2]. Explicit analytical solutions for $\beta_i = \beta_i(\kappa_i)$, $i = 1, 2$, are available [8,9], but they must be treated with care because of sign ambiguities.

C. Sun–Earth Dihedral Angle

The geometry of the sun and Earth measurements shown in Fig. 1 generates another independent measurement, namely the sun–Earth dihedral angle α, see also Wertz [5], section 7.3. This angle is derived from the measurement of the time interval between the sun's crossing of the sun sensor's vertical slit and the Earth sensor observing the Earth-center crossing (which follows from the mean value of the S/E and E/S crossing pulses). To minimize the bias effects, the average of the two results generated by each of the two pencil-beams should be used in practice [2].

The spherical geometry in the triangle formed by the **S**, **E**, and **Z** unit vectors in Fig. 1 produces a rather intricate nonlinear measurement equation between α and the attitude **Z** and involves the measurement angles ϑ and β:

$$\alpha(\nu) = \arcsin\{\mathbf{Z} \bullet (\mathbf{S} \times \mathbf{E})/(\sin\vartheta \sin\beta)\} \tag{4}$$

It should be noted that both angles ϑ and β must stay away from the singularities for 0 and 180° in Eq. (4). This implies that the spin-axis attitude vector should not be aligned with the sun or Earth direction. In fact, this singularity is not just mathematical in nature but also mechanical because, in these singularity cases, the sun (or Earth) sensor is not able to generate the angular measurements needed for the sun (or Earth) aspect angle calculations. Provided that also the sun and Earth vectors are not aligned we can see that the α angle in Eq. (4) is well defined.

For the subsequent analyses it is advantageous to use the auxiliary angle γ defined by:

$$\gamma = \arccos\{\sin\vartheta \sin\beta \sin\alpha / \sin\psi\} \tag{5}$$

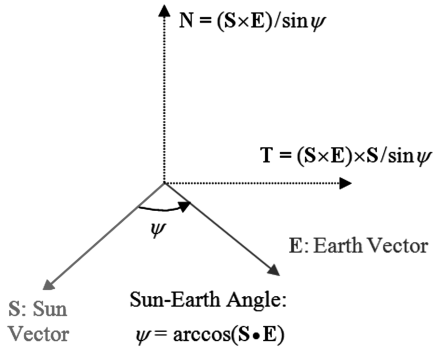

Fig. 2 Definition of sun–Earth angle ψ and N, T unit vectors.

where the angle ψ (with $0 \le \psi \le 180°$) refers to the sun–Earth angle shown in Fig. 2:

$$\psi(\nu) = \arccos\{\mathbf{S} \bullet \mathbf{E}(\nu)\} \tag{6}$$

Next, we introduce the unit vector **N**, which points normal to both **S** and **E** vectors (Fig. 2):

$$\mathbf{N} = (\mathbf{S} \times \mathbf{E})/|\mathbf{S} \times \mathbf{E}| = (\mathbf{S} \times \mathbf{E})/\sin\psi \tag{7}$$

After these preliminaries it is possible to express Eq. (5) in the more favorable form:

$$\gamma = \arccos\{\mathbf{Z} \bullet \mathbf{N}\} \tag{8}$$

which has the same simple structure as Eqs. (1) and (2).

D. System of Measurement Equations

We can now describe the relationships in Eqs. (1), (2), and (8) between the observation angles ϑ, β, γ, and the attitude vector **Z** in terms of a three-dimensional linear system of equations as follows:

$$\mathbf{y} = H\mathbf{Z} \tag{9a}$$

with:

$$\mathbf{y} = \begin{pmatrix} \cos\vartheta \\ \cos\beta \\ \cos\gamma \end{pmatrix} \tag{9b}$$

$$H = \begin{bmatrix} S_1 & S_2 & S_3 \\ E_1 & E_2 & E_3 \\ N_1 & N_2 & N_3 \end{bmatrix} \tag{9c}$$

The subscripts 1, 2, and 3 refer to the components of the respective vectors along the coordinate axes of the adopted inertial reference frame:

$$\mathbf{S} = (S_1, S_2, S_3)^\top \tag{10a}$$

$$\mathbf{E} = (E_1, E_2, E_3)^\top \tag{10b}$$

$$\mathbf{N} = ((\mathbf{S} \times \mathbf{E})_1, (\mathbf{S} \times \mathbf{E})_2, (\mathbf{S} \times \mathbf{E})_3)^\top / \sin\psi \tag{10c}$$

III. Single-Frame Attitude Solution

The system of Eqs. (9) becomes ill-defined when the reference unit vectors **S** and **E** are aligned (i.e., if $\psi = 0$ or 180°). Away from these singularity conditions, the unique attitude solution can immediately be obtained from Eqs. (9) by inverting the nonsingular matrix H:

$$\mathbf{Z}_{\text{sf}} = H^{-1}\mathbf{y} \tag{11}$$

The vector $\mathbf{Z}_{sf}$ represents the deterministic *single-frame* attitude solution because all three individual measurement angles ϑ, β, and γ should be collected at a single identical instant of time (i.e., within the same spin revolution). Because of the measurement errors, the resulting attitude solution $\mathbf{Z}_{sf}$ does in general not have unit magnitude. Therefore, unit-vector normalization should be performed subsequently, see [9,10].

An interesting and more illustrative alternative form of the single-frame solution $\mathbf{Z}_{sf}$ can be established by introducing the auxiliary 3×3 dimensional matrix P_0 defined by:

$$P_0 = [H^\top H]^{-1} = [\mathbf{S}\mathbf{S}^\top + \mathbf{E}\mathbf{E}^\top + \mathbf{N}\mathbf{N}^\top]^{-1} = \begin{bmatrix} S_1^2 + E_1^2 + N_1^2 & S_1S_2 + E_1E_2 + N_1N_2 & S_1S_3 + E_1E_3 + N_1N_3 \\ S_1S_2 + E_1E_2 + N_1N_2 & S_2^2 + E_2^2 + N_2^2 & S_2S_3 + E_2E_3 + N_2N_3 \\ S_1S_3 + E_1E_3 + N_1N_3 & S_2S_3 + E_2E_3 + N_2N_3 & S_3^2 + E_3^2 + N_3^2 \end{bmatrix}^{-1} \tag{12}$$

It can be shown that the matrix P_0 is well defined as long as H is nonsingular.

The matrix P_0 enables us to write the single-frame attitude solution $\mathbf{Z}_{sf}$ of Eq. (11) in a more meaningful form that shows its components along the directions $\mathbf{S}$, $\mathbf{E}$, $\mathbf{N}$ in an explicit manner as follows:

$$\mathbf{Z}_{sf} = H^{-1}\mathbf{y} = P_0P_0^{-1}H^{-1}\mathbf{y} = P_0H^\top\mathbf{y} \tag{13a}$$

$$\Rightarrow \mathbf{Z}_{sf} = P_0\{\cos\vartheta\,\mathbf{S} + \cos\beta\,\mathbf{E} + \cos\gamma\,\mathbf{N}\} \tag{13b}$$

The manipulations described by Eqs. (12) and (13) represent the mechanization of the Moore–Penrose pseudoinverse of the matrix H, which arises naturally in least-squares solutions (see also the next section).

The solution in Eq. (13b) can best be visualized in the case when the reference axes $\mathbf{S}$, $\mathbf{E}$, $\mathbf{N}$ are normal to each other and the attitude vector has equal projections of $\sqrt{3}/3$ on each of these axes. In this special case, all angles ϑ, β, and γ are equal to $\cos^{-1}(\sqrt{3}/3) \approx 54.7°$ and P_0 degenerates to the identity matrix.

IV. Formal Least-Squares Attitude Solutions

A. System of Equations

In practical applications [1,2], a large batch of m sets of angular measurements ϑ_j, β_j, α_j $(j = 1, \ldots, m)$ is collected over m spin periods. This produces the $3m$-dimensional measurement vector $\mathbf{y}$ and the system of equations consists of m times the three single-frame measurement equations of Eq. (9). However, this system of equations is overdetermined as it possesses only three unknowns, i.e., the components of the attitude $\mathbf{Z}$. Therefore, the unknown random errors $\mathbf{v} = (\nu_1, \ldots, \nu_{3m})^\top$ are added to the $3m$ measurement equations of Eqs. (9) and we have:

$$\mathbf{y} = H\mathbf{Z} + \mathbf{v} \tag{14}$$

where the measurement matrix H has now the dimension $3m \times 3$.

This formulation enables us to determine the least-square estimate [11] of the attitude vector $\mathbf{Z}^*$ from the overdetermined system of $3m$ measurement equations.

B. Straightforward Least-Squares Attitude Solution

The most straightforward LS approach considers the $3m$-dimensional vector $\mathbf{y}$ under the assumption that all m measurements are considered to be uncorrelated and to carry identical weights. In this case, the measurement covariance matrix is expressed as:

$$R = E\{\Delta\mathbf{y}(\Delta\mathbf{y})^\top\} = E\{\mathbf{v}\mathbf{v}^\top\} = \sigma^2 I \tag{15}$$

where σ^2 stands for $E\{\nu_j^2\}$, $j = 1, \ldots, 3m$, and I denotes the $3m \times 3m$ identity matrix.

The least-squares estimate corresponds to the attitude solution $\mathbf{Z}^*$ that minimizes the sum of the squares of the measurement residuals expressed by the cost function:

$$J = (\mathbf{y} - H\mathbf{Z})^\top(\mathbf{y} - H\mathbf{Z}) \tag{16}$$

The optimal estimate that minimizes this cost function is written as $\mathbf{Z}^*$ and can be expressed in terms of the $3m$-dimensional measurement vector $\mathbf{y}$ as follows:

$$\mathbf{Z}^* = PH^\top\mathbf{y} \tag{17a}$$

$$\text{with} \quad P = [H^\top H]^{-1} \tag{17b}$$

where the 3×3 matrix P represents a generalization of the matrix P_0 introduced in Eq. (12):

$$P = \left\{\sum_{j=1}^{m}[P_j]^{-1}\right\}^{-1} = \left\{\sum_{j=1}^{m}[\mathbf{S}_j\mathbf{S}_j^\top + \mathbf{E}_j\mathbf{E}_j^\top + \mathbf{N}_j\mathbf{N}_j^\top]\right\}^{-1} \tag{18}$$

The matrices P_j are defined in a similar way as P_0 in Eq. (12) but for each of the m individual reference vectors $\mathbf{S}_j$, $\mathbf{E}_j$, and $\mathbf{N}_j$ at the successive measurement times t_j $(j = 1, 2, \ldots, m)$.

The LS estimate $\mathbf{Z}^*$ in Eq. (17a) can now be expressed in the form:

$$\mathbf{Z}^* = P\sum_{j=1}^{m}\{\cos\vartheta_j\mathbf{S}_j + \cos\beta_j\mathbf{E}_j + \cos\gamma_j\mathbf{N}_j\} \tag{19}$$

The similarity between this result and the single-frame attitude solution in Eq. (13b) is self-evident and can easily be interpreted.

The symmetric 3×3 covariance matrix of the attitude estimation error $\Delta\mathbf{Z} = \mathbf{Z}^* - \mathbf{Z}$ in Eq. (19) can now be calculated directly from Eq. (17a) while employing Eqs. (15) and (17b):

$$E\{\Delta\mathbf{Z}(\Delta\mathbf{Z})^\top\} = PH^\top E\{\Delta\mathbf{y}(\Delta\mathbf{y})^\top\}HP^\top = \sigma^2 P \tag{20}$$

This confirms that the matrix P defined in Eq. (17b) is strongly related to the error covariance matrix of the straightforward least-square attitude estimate $\mathbf{Z}^*$.

C. Uncorrelated Weighted-Least-Squares Attitude Solution

Next, we study the case when the three angular observations ϑ, β, and γ are given different weights but are still considered to be uncorrelated with respect to each other. In this case, the measurement covariance matrix R of Eq. (15) has nonzero terms only on its diagonal, but they are different, and repeat in groups of three terms as follows:

$$R = E\{\Delta\mathbf{y}(\Delta\mathbf{y})^\top\} = \begin{bmatrix} \sigma_1^2 & 0 & 0 & 0 & \ldots & 0 \\ 0 & \sigma_2^2 & 0 & 0 & \ldots & 0 \\ 0 & 0 & \sigma_3^2 & 0 & \ldots & 0 \\ 0 & 0 & 0 & \sigma_1^2 & \ldots & 0 \\ \vdots & \vdots & \vdots & \vdots & \ldots & \vdots \\ 0 & 0 & 0 & 0 & \ldots & \sigma_3^2 \end{bmatrix} \tag{21}$$

The cost function for the weighted-least-squares (WLS) problem is usually expressed as:

$$J = (\mathbf{y} - H\mathbf{Z})^\top W(\mathbf{y} - H\mathbf{Z}) \tag{22}$$

where the weighting matrix W corresponds to the inverse of the measurement covariance matrix defined in Eq. (21), i.e., $W = R^{-1}$.

The WLS estimate of the attitude vector can be established similarly as in Eqs. (17):

$$\mathbf{Z}^* = QH^\top R^{-1}\mathbf{y} \tag{23a}$$

$$\text{with: } Q = [H^\top R^{-1} H]^{-1} \tag{23b}$$

This WLS attitude estimate can readily be expressed in the following explicit form:

$$\mathbf{Z}^* = Q\sum_{j=1}^{m}\left\{\frac{\cos\vartheta_j}{\sigma_1^2}\mathbf{S}_j + \frac{\cos\beta_j}{\sigma_2^2}\mathbf{E}_j + \frac{\cos\gamma_j}{\sigma_3^2}\mathbf{N}_j\right\} \tag{24}$$

which represents an obvious generalization of the result established in Eq. (19).

The error covariance matrix Q of the estimate $\mathbf{Z}^*$ defined in Eq. (23b) can be written in the following explicit form:

$$Q = \left\{\sum_{j=1}^{m}\left[\frac{\mathbf{S}_j\mathbf{S}_j^\top}{\sigma_1^2} + \frac{\mathbf{E}_j\mathbf{E}_j^\top}{\sigma_2^2} + \frac{\mathbf{N}_j\mathbf{N}_j^\top}{\sigma_3^2}\right]\right\}^{-1} \tag{25}$$

The correspondence between the results of Eq. (25) and the less general result in Eq. (18) is self-evident.

The efficient and practically useful least-squares solutions for the spin-axis attitude and its covariances presented in Eqs. (24) and (25) were first established by Shuster in [3], Eqs. (45). A more recent paper [10] presents many additional results, in particular for enforcing the unit-vector constraint of the attitude vector.

D. General Weighted-Least-Squares Attitude Solution

The general weighted-least-squares problem considers measurements that not only carry different weights but may also be correlated to each other. The general error measurement matrix takes the form:

$$R = E\{\Delta\mathbf{v}(\Delta\mathbf{v})^\top\} = \begin{bmatrix} \sigma_1^2 & \sigma_{12} & \sigma_{13} & \dots & \sigma_{1,3m} \\ \sigma_{21} & \sigma_2^2 & \sigma_{23} & \dots & \sigma_{2,3m} \\ \sigma_{31} & \sigma_{32} & \sigma_3^2 & \dots & \sigma_{3,3m} \\ \vdots & \vdots & \vdots & \dots & \vdots \\ \sigma_{3m,1} & \sigma_{3m,2} & \sigma_{3m,3} & \dots & \sigma_{3m,3m}^2 \end{bmatrix} \tag{26}$$

This represents a symmetric $3m \times 3m$ matrix because $\sigma_{jk} = \sigma_{kj}$ for j, $k = 1, 2, \dots, 3m$.

The optimal attitude estimate $\mathbf{Z}^*$ and its covariance matrix Q may formally be established by means of the relationships given in Eqs. (23). However, these results would become more complicated because the measurement covariance matrix R in Eq. (26) induces nondiagonal terms in the state covariance matrix Q. Therefore, attractive explicit analytical expressions like those in Eqs. (24) and (25) cannot be established in the general case.

V. Covariances of Sun–Earth Sensor Measurements

In this section we determine and analyze the elements of the general error covariance matrix R defined in Eq. (26) for typical sun and Earth sensor measurements while accounting for the actual correlations between these measurements. Equation (4) suggests that the errors in the sun–Earth dihedral angle α would be correlated with those of both the sun- and Earth-aspect angles ϑ and β. However, the actual algorithmic processing of the fundamental sensor crossing pulses should be taken into account when calculating the measurement covariances.

The sun and Earth sensors use different hardware measurement devices and different processing approaches. Therefore, the random measurement errors of the sun-aspect angle ϑ are uncorrelated from those of the Earth-aspect angle measurement and the correlation terms between the angular measurements ϑ and β can be expected to vanish. This is indeed confirmed by the result of the covariance matrix in Eq. (39) of [9]. Similarly, although not as obvious, also the correlation terms between the angular measurements β and α vanish, see Eq. (39) of [9]. On the other hand, however, Eq. (39) of [9] shows that the correlation terms between the ϑ and α angular measurements do not vanish.

We now proceed to calculate the covariances of the observation vector $\mathbf{y}$ in terms of the errors of the angular measurements ϑ, β, and α. First, we establish the error propagation from the angular measurements to the vector $\mathbf{y}$ by using Eq. (9b):

$$\Delta\mathbf{y} \approx F\begin{pmatrix} \Delta\vartheta \\ \Delta\beta \\ \Delta\alpha \end{pmatrix} \tag{27a}$$

$$\text{with: } F = \begin{bmatrix} -\sin\vartheta & 0 & 0 \\ 0 & -\sin\beta & 0 \\ f_1 & f_2 & f_3 \end{bmatrix} \tag{27b}$$

The functions f_j are defined by:

$$f_j = g_j/\sin\psi \qquad (j = 1, 2, 3) \tag{28}$$

with:

$$g_1 = \cos\vartheta\sin\beta\sin\alpha \tag{29a}$$

$$g_2 = \sin\vartheta\cos\beta\sin\alpha \tag{29b}$$

$$g_3 = \sin\vartheta\sin\beta\cos\alpha \tag{29c}$$

The angle ψ refers to the sun–Earth angle defined in Eq. (6) and shown in Fig. 2. The expressions in Eqs. (27–29) show a singularity for $\psi \to 0, 180°$ corresponding to the situations when the sun and Earth vectors become aligned. In these cases, the matrix H in Eq. (9c) becomes singular and a unique attitude solution cannot be established.

We assume that measurements taken at different instants of time t_j and t_k $(j \neq k)$ are independent. Therefore, correlations can only occur for the three angular measurements taken at the same instant t_j for $j = 1, 2, \dots, m$.

When executing the covariance transformation from the angles ϑ, β, and α to the vector $\mathbf{y}$ at each measurement instant t_j $(j = 1, 2, \dots, m)$ we find that the $3m \times 3m$ matrix R in Eq. (26) contains the following m times 3×3 nonzero blocks around its diagonal:

$$R_{3\times3} = E\{\Delta\mathbf{y}(\Delta\mathbf{y})^\top\} = \begin{bmatrix} \sigma_1^2 & 0 & \sigma_{13} \\ 0 & \sigma_2^2 & \sigma_{23} \\ \sigma_{13} & \sigma_{23} & \sigma_3^2 \end{bmatrix} \tag{30}$$

The entries in this matrix depend on the measurement angles ϑ, β, α, and their covariances and can be calculated from Eqs. (27–29):

$$\sigma_1^2 = \sigma_\vartheta^2\sin^2\vartheta \tag{31a}$$

$$\sigma_2^2 = \sigma_\beta^2\sin^2\beta \tag{31b}$$

$$\sigma_3^2 = G_3^2/\sin^2\psi \tag{31c}$$

$$\sigma_{13} = -G_{13}/\sin\psi \tag{31d}$$

$$\sigma_{23} = -G_{23}/\sin\psi \tag{31e}$$

with:

$$G_3^2 = g_1^2\,\sigma_\vartheta^2 + g_2^2\,\sigma_\beta^2 + g_3^2\,\sigma_\alpha^2 + 2g_1g_3\,\sigma_{\vartheta\alpha} \tag{32a}$$

$$G_{13} = (g_1\ \sigma_\vartheta^2 + g_3\ \sigma_{\vartheta\alpha})\sin\vartheta \tag{32b}$$

$$G_{23} = g_2\ \sigma_\beta^2 \sin\beta \tag{32c}$$

Finally, the attitude covariance matrix Q defined in Eq. (23b) should be expressed in terms of the elements of the general measurement covariance matrix $R_{3\times3}$ in Eq. (30). First, the inverse of the measurement covariance matrix $R_{3\times3}$ can be established as:

$$[R_{3\times3}]^{-1} = \frac{1}{D}\begin{bmatrix} (\sigma_2\sigma_3)^2 - \sigma_{23}^2 & \sigma_{13}\sigma_{23} & -\sigma_{13}\sigma_2^2 \\ \sigma_{13}\sigma_{23} & (\sigma_1\sigma_3)^2 - \sigma_{13}^2 & -\sigma_{23}\sigma_1^2 \\ -\sigma_{13}\sigma_2^2 & -\sigma_{23}\sigma_1^2 & (\sigma_1\sigma_2)^2 \end{bmatrix} \tag{33}$$

where D is the determinant of the covariance matrix $R_{3\times3}$. It may be noted that D represents the volume of the three-dimensional covariance ellipsoid:

$$D = \{(\sigma_1\sigma_2\sigma_3)^2 - \sigma_{23}^2\sigma_1^2 - \sigma_{13}^2\sigma_2^2\} \tag{34}$$

This expression for D confirms that the correlation terms of the derived measurements y_1 and y_2 with respect to y_3 reduce the size of the measurement covariance ellipsoid.

When substituting the results of Eqs. (31) and (32) into Eq. (33) we obtain:

$$[R_{3\times3}]^{-1} = \frac{1}{Ds^2}\begin{bmatrix} (G_3\sigma_2)^2 - G_{23}^2 & G_{13}G_{23} & sG_{13}\sigma_2^2 \\ G_{13}G_{23} & (G_3\sigma_1)^2 - G_{13}^2 & sG_{23}\sigma_1^2 \\ sG_{13}\sigma_2^2 & sG_{23}\sigma_1^2 & (\sigma_1\sigma_2)^2 \end{bmatrix} \tag{35}$$

with:

$$s = \sin\psi \tag{36a}$$

$$D = \{(G_3\sigma_1\sigma_2)^2 - G_{23}^2\sigma_1^2 - G_{13}^2\sigma_2^2\}/s^2 \tag{36b}$$

This result shows that the size of the measurement covariance matrix is minimal when the sun–Earth angle $\psi = 90°$. On the other hand, the volume grows without bounds when the sun and Earth directions approach alignment, i.e., when $\psi \to 0$ or $180°$.

Afterward, the state covariance matrix Q may be calculated from the expression in Eq. (23b), at least in principle, by using the knowledge of the H matrix in Eq. (9c). It is evident that the analytical calculations become intimidating at this stage. Therefore, a different approach will be pursued in the next section.

VI. Attitude Estimation in Local Frame

A. Background and Motivation

The results presented in Eqs. (24) and (25) represent explicit analytical expressions for the attitude estimate and its covariance matrix in terms of the inertial representations of the **S**, **E**, and **N** reference unit vectors. These expressions are valid in the special case when the measurement covariance matrix is diagonal as illustrated in Eq. (21). As concluded in the previous section, it is much more tedious to establish the explicit analytical results for the general measurement covariance matrix in Eq. (26).

In any case, the general covariance results established above cannot immediately be interpreted in terms of their geometrical singularities. More informative insights may be found by representing the attitude vector and the measurement equations in terms of the local orthogonal coordinate frame defined by the orthogonal unit vectors **S**, **T**, **N** shown in Fig. 2.

The orthogonal rotation matrix A from the inertial frame to the local coordinate frame is defined as follows:

$$\begin{pmatrix} S \\ T \\ N \end{pmatrix}_{\text{Local}} = A\begin{pmatrix} X \\ Y \\ Z \end{pmatrix}_{\text{Inertial}} \quad \text{with: } A = \begin{bmatrix} S_1 & S_2 & S_3 \\ T_1 & T_2 & T_3 \\ N_1 & N_2 & N_3 \end{bmatrix} \tag{37}$$

The inverse matrix $A^{-1} = A^\top$ represents the inverse coordinate transformation.

It is important to note that the local reference frame defined by the **S**, **T**, **N** unit vectors does not remain fixed in inertial space. The sun vector moves about 1° per day, so that the maximum deviation in the sun position is about $\pm0.02°$ from the central value for a one-hour batch of sensor data. Therefore, the motion of the sun vector may be neglected for short data intervals of up to 1 h.

The Earth vector, on the other hand, moves much faster because it rotates along with the orbital radius vector. When considering a geostationary satellite, for instance, the rate of change of the Earth-vector is as much as 15° per hour. This means that deviations in the Earth-vector position would reach the limit of $\pm0.02°$ already at the beginning and end of a 10-s interval of sensor data.

Nevertheless, a satellite with a spin-rate of 60 (or 100) rpm generates a batch of 10 (or 16) independent measurements within a 10-s interval. Furthermore, after each 10-s interval we may update (i.e., rectify) the **S**, **T**, and **N** reference axes and the associated transformation matrix A. Therefore, by using this strategy, it is possible to keep the errors for large batches of data (consisting of a sequence of 10-s intervals) within acceptable limits.

Regardless of the practical issues that need to be taken into account when employing the local coordinate frame for attitude determination, our most important motivation for the adoption of this frame is to gain deeper insights into the characteristics of the attitude determination singularities that are hard to evaluate within the common inertial formulation.

B. Measurement Equations

We introduce the attitude vector **z** in terms of its components along the local coordinate axes:

$$\mathbf{z} = (z_1, z_2, z_3)^\top = z_1\mathbf{S} + z_2\mathbf{T} + z_3\mathbf{N} \tag{38}$$

The system of measurement equations in Eqs. (9) can now be replaced by the simpler system:

$$\mathbf{y} = \begin{pmatrix} \cos\theta \\ \cos\beta \\ \cos\gamma \end{pmatrix} = h\begin{pmatrix} z_1 \\ z_2 \\ z_3 \end{pmatrix} \tag{39a}$$

$$\text{with: } h = \begin{bmatrix} 1 & 0 & 0 \\ \cos\psi & \sin\psi & 0 \\ 0 & 0 & 1 \end{bmatrix} \tag{39b}$$

This result indicates that the local measurement matrix h depends only on the instantaneous sun–Earth angle ψ.

The inverse of the matrix h can readily be calculated as:

$$h^{-1} = \frac{1}{\sin\psi}\begin{bmatrix} \sin\psi & 0 & 0 \\ -\cos\psi & 1 & 0 \\ 0 & 0 & \sin\psi \end{bmatrix} \tag{40}$$

which explicitly shows the singularity in the case when $\psi \to 0, 180°$ in the first two terms of the second row of h^{-1}. In these cases, the sun and Earth vectors are aligned so that the first two measurement equations are no longer independent.

C. Single-Frame Attitude Solution

The single-frame attitude solution $\mathbf{z}_{\text{sf}}$ in the local **S**, **T**, **N** frame shown in Fig. 2 can readily be established in explicit form by employing the inverse matrix h^{-1} in Eq. (40):

$$\mathbf{z}_{\text{sf}} = h^{-1}\mathbf{y} = \begin{pmatrix} \cos\theta \\ (\cos\beta - \cos\psi\cos\theta)/\sin\psi \\ \cos\gamma \end{pmatrix} \tag{41}$$

This result confirms the presence of the singularities in the second component of the attitude solution $\mathbf{z}_{\text{sf}}$ for $\psi \to 0, 180°$. Also we see that, in the special case when $\psi = 90°$, the single-frame attitude

solution $\mathbf{z}_{sf}$ in Eq. (41) becomes identical to the measurement vector $\mathbf{y}$. This special case may also be visualized from the sun–Earth geometry shown in Fig. 2.

It is of interest to establish the equivalent of the alternative single-frame solution presented in Eqs. (12) and (13). Thereto, in analogy with the matrix P_0, we first introduce the auxiliary matrix p_0 as follows:

$$p_0 = [h^\top h]^{-1} = \begin{bmatrix} 1 & -c/s & 0 \\ -c/s & (1+c^2)/s^2 & 0 \\ 0 & 0 & 1 \end{bmatrix} \tag{42a}$$

with:

$$c = \cos\psi; \qquad s = \sin\psi \tag{42b}$$

It can be confirmed by explicit calculation that the single-frame solution in Eq. (41) may also be written in the form:

$$\mathbf{z}_{sf} = p_0 h^\top \mathbf{y} = p_0 \begin{pmatrix} \cos\vartheta + c\cos\beta \\ s\cos\beta \\ \cos\gamma \end{pmatrix} \tag{43}$$

which represents the counterpart of Eq. (13b) in the inertial case. In the special case when $\psi = 90°$ the result in Eq. (43) degenerates into $\mathbf{z}_{sf} = \mathbf{y}$ as expected.

D. LS Local Attitude Solutions

The straightforward LS estimate $\mathbf{z}^*$ can also be calculated from the batch of measurement data in a similar way as was done in Eqs. (17) and (18):

$$\mathbf{z}^* = p h^\top \mathbf{y} \tag{44}$$

with:

$$p = \left\{ \sum_{j=1}^{k} [p_j]^{-1} \right\}^{-1} = \left\{ \sum_{j=1}^{k} [h_j^\top h_j] \right\}^{-1} \tag{45}$$

The index k in Eq. (45) takes the place of the index m used in Eq. (18) of the inertial formulation. It represents the upper index of the sequence of measurement data collected at t_j ($j = 1, 2, \ldots, k$, with $k \ll m$ in general) within the 10-s interval during which the adopted local coordinate frame remains valid.

The matrices p_j ($j = 1, 2, \ldots, k$) are defined similarly as in Eq. (42a) at each of the sampling instants t_j. However, because the sun and Earth positions are kept fixed during each 10-s data interval, all matrices p_j ($j = 1, 2, \ldots, k$) are identical during the short interval under consideration, so we can write:

$$p_j = [h^\top h]^{-1} = \begin{bmatrix} 1 & -c/s & 0 \\ -c/s & (1+c^2)/s^2 & 0 \\ 0 & 0 & 1 \end{bmatrix} \quad \text{for } j = 1, 2, \ldots, k \tag{46}$$

This leads to a very compact and attractive result for the matrix p in Eq. (45):

$$p = \left\{ \sum_{j=1}^{k} [p_j]^{-1} \right\}^{-1} = \frac{1}{k} [h^\top h]^{-1} = \frac{1}{k} p_0 \tag{47}$$

The local LS attitude estimate $\mathbf{z}^*$ in Eq. (44) takes the place of the inertial attitude estimate $\mathbf{Z}^*$ in Eq. (17a). The covariance matrix of the estimate $\mathbf{z}^*$ can readily be calculated and the result equals the product of the angular measurement covariance σ^2 and the matrix p in Eq. (47) similarly as in Eq. (20).

The local results presented here are more compact than the inertial formulations in Eqs. (17) and (18). Also they have the advantage that the measurement and covariance matrices remain constant over the short intervals considered here.

E. General LS Local Attitude Solutions

In the most general case, the attitude covariance matrix q of the local WLS attitude estimate is introduced to replace the matrix Q defined in Eq. (23b). This matrix can be expressed in terms of the measurement covariance matrix R in Eq. (30), while using the simpler expressions for the h and h^{-1} matrices defined in Eqs. (39b) and (40). The explicit result for q takes the form:

$$\begin{aligned} q &= [h^\top R^{-1} h]^{-1} \\ &= \frac{1}{k} \begin{bmatrix} \sigma_1^2 & -c\sigma_1^2/s & -G_{13}/s \\ -c\sigma_1^2/s & (\sigma_2^2 + c^2\sigma_1^2)/s^2 & (cG_{13} - G_{23})/s^2 \\ -G_{13}/s & (cG_{13} - G_{23})/s^2 & G_3^2/s^2 \end{bmatrix} \end{aligned} \tag{48}$$

The determinant of the matrix q represents the volume of the three-dimensional covariance ellipsoid associated with the expected attitude error and can be calculated as:

$$\det(q) = \{(G_3\sigma_1\sigma_2)^2 - G_{23}^2\sigma_1^2 - G_{13}^2\sigma_2^2\}/(ks^4) = D/(ks^2) \tag{49}$$

It follows that the determinant D of the covariance matrix q as a function of the sun–Earth angle is identical (apart from the factor $1/k$) to the determinant of the measurement covariance matrix $R_{3\times3}$ as can be seen from Eqs. (34) and (36b).

As usual, it is possible to simplify the attitude covariance matrix in Eq. (48) by introducing a coordinate transformation to principal axes. This simplifies the structure of the matrix q in the sense that the off-diagonal terms vanish and only the diagonal nonzero terms (i.e., the eigenvalues of q) remain. However, the calculation of the eigenvalues of q in Eq. (48) is fairly daunting and provides little additional useful information.

F. Expected Attitude Determination Error

It is interesting and useful to interpret the mathematical results for the covariances in terms of the expected attitude (determination) error, i.e., the difference between the estimated and actual attitude pointing directions.

The expected attitude error σ_{att} is defined as:

$$\sigma_{att} = E\{|\Delta\mathbf{Z}|\} \tag{50a}$$

$$\Rightarrow \sigma_{att} \le \sqrt{\sum_{k=1}^{3} E\{(\Delta Z_k)^2\}} \tag{50b}$$

This result follows from the application of Jensen's inequality to the concave square-root function and provides a convenient conservative upper bound for the expected attitude error.

Similarly, the attitude error may also be written in terms of its components along the local reference frame defined by the **S**, **T**, **N** unit vectors. When recalling the definition of the attitude covariance matrix in Eq. (48) we can express the expected attitude error σ_{att} in terms of the elements of the covariance matrix q as follows:

$$\sigma_{att} \le \sqrt{\text{trace}(q)} \tag{51}$$

where trace q denotes the sum of the diagonal terms of matrix q.

When substituting the elements of q in Eq. (48) we find:

$$\sigma_{att} \le \frac{1}{\sin\psi} \sqrt{\{\sigma_1^2 + \sigma_2^2 + G_3^2\}/k} \tag{52}$$

This result reveals the explicit dependence of the attitude error on the sun–Earth angle ψ in terms of the nature of the singularity for $\psi \to 0$ and 180°.

VII. Application to Real Missions

We illustrate the covariance results established above for two actual satellite missions, i.e., CONTOUR [2,9], and MSG-2 [8] with very different orbit and attitude characteristics.

Table 1 Range of angles over one-hour interval of sensor data (CONTOUR)

Angle	Initial value, deg	Final value, deg
Spin-axis attitude (constant)	RA = 258.6; DE = 29.2	
Sun-aspect angle ϑ	104.07	104.07
Earth-aspect angle β	64.23	60.06
Sun–Earth dihedral angle α	36.69	36.69
Sun-–Earth angle ψ	53.51	56.45

Table 2 Variation of angles over selected interval of sensor data (MSG-2)

Angle	Initial value, deg	Final value, deg
Spin-axis attitude (constant)	RA = 83.8; DE = 86.5	
Sun-aspect angle ϑ	115.56	116.46
Earth-aspect angle β	93.50	86.50
Sun–Earth dihedral angle α	varies over full 360° range	
Sun–Earth angle ψ	24.13 (min)	155.8 (max)

A. CONTOUR Application

In the case of CONTOUR, precise attitude determination was required for the injection (by means of a solid-rocket motor) from its Earth-phasing orbit into a heliocentric trajectory in August 2002. The perigee and apogee distances were about 200 and 116,000 km, respectively, and the orbital period was almost 42 hours. Because the injection was performed at perigee, the spin-axis attitude orientation was close to the perigee velocity vector. The Earth sensor's pencil-beams had simultaneous Earth coverage over the altitude range from about 45,000 to 60,000 km starting from about 15 hours after apogee passage.

The most suitable interval for collecting sensor data for attitude determination purposes occurs when the Earth sensor's pencil-beams scan the Earth's rim in the midlatitude region defined in [2] and this interval is about 1 h in duration.

Table 1 summarizes the variations of the geometrical angles over the relevant one-hour interval. The spin-axis attitude can be taken constant over this short period and is given by its right ascension (RA) and declination (DE) angles. The sun-aspect angle ϑ and the dihedral angle α also remain essentially constant, but the sun–Earth angle ψ and the Earth-aspect angle β vary by about 3–4°.

The variation of the expected attitude error of Eq. (52) as a function of the sun–Earth angle ψ is illustrated in Fig. 3. This shows that the minimum expected error occurs for $\psi = 90°$ as expected.

The input values used in Fig. 3 are calculated from the random error model established in [9], i.e., $\sigma_\vartheta = 0.0026°$, $\sigma_\beta = 0.014°$, $\sigma_\alpha = 0.0061°$, and $\rho_{\vartheta\alpha} = 0.1$. The results are not at all sensitive to variations in the correlation coefficient $\rho_{\vartheta\alpha}$ of the ϑ and α measurements.

The one-hour interval of collected sensor data used in Table 1 is relatively favorable in terms of the expected attitude error as it is far away from the singularities at $\psi = 0$ and 180°.

B. MSG-2 Application

The second case studied is the METEOSAT Second Generation (MSG-2) satellite during its near-geostationary drift phase in December 2005, see also [8,9]. The MSG satellites have a spin-axis attitude orientation that points close to the orbit-normal. This means that the Earth-aspect angle remains near 90° (i.e., within a fraction of a degree) and the Earth sensor's pencil-beams have continuous Earth coverage throughout the orbit.

The Earth sensor's pencil-beams continuously scan the Earth's rim in the midlatitude region [8] so that full-day intervals of sensor data may be selected for attitude determination purposes. The spin-axis attitude can be taken constant over the 24-hour period and is specified in Table 2 in terms of its RA and DE angles. Table 2 also gives the boundaries of the relevant angles over this one-day period. As in Table 1, the variations of the sun- and Earth-aspect angles are relatively minor, but the variations of the sun–Earth angle ψ and the dihedral angle α are much larger in this case.

The behavior of the expected attitude error in Eq. (52) as a function of the sun–Earth angle ψ is illustrated in Fig. 4. Although the evolution of the attitude error may look identical to the one shown in Fig. 3, the very different geometry has been accounted for. As in the previous example, the minimum expected error occurs at $\psi = 90°$ as expected. The range of the sun–Earth angle variations is almost 132° and is much larger than in the CONTOUR case. This is due to the fact that the Earth sensor has continuous coverage during the 24-hour period geostationary orbit.

The input values used here are calculated from the random error model presented previously [9] and are slightly different from the CONTOUR case, i.e., $\sigma_\vartheta = 0.0022°$, $\sigma_\beta = 0.015°$, $\sigma_\alpha = 0.0061°$, and $\rho_{\vartheta\alpha} = 0.1$.

Although the attitude determination interval is much longer than in CONTOUR's case, the expected attitude error remains favorable because the sun–Earth angle keeps a good distance away from the singularities at $\psi = 0$, 180° throughout the one-day interval.

Finally, it should be noted that the attitude errors in Figs. 3 and 4 are calculated by using only one measurement (i.e., $k = 1$). When using larger data batches, we can essentially eliminate the random noise effect. In practice, however, unknown biases have a much more severe effect on the attitude error than random errors have, see also [12].

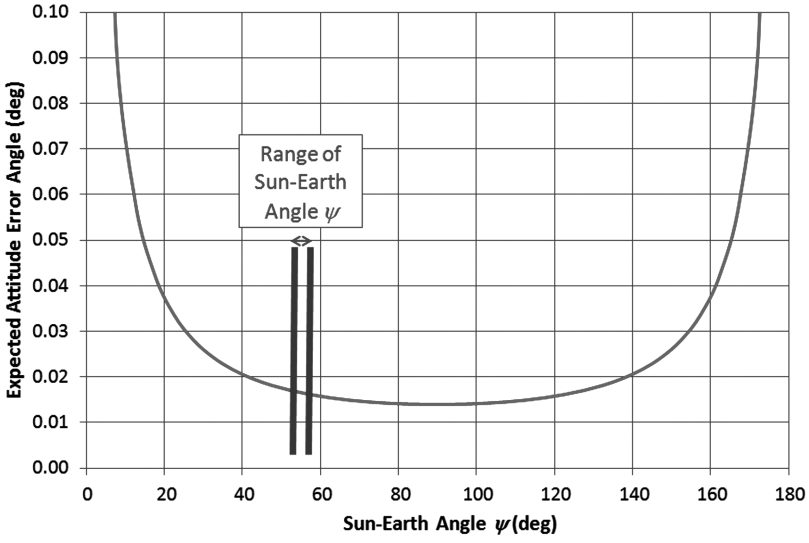

Fig. 3 Expected attitude error as function of the sun–Earth angle (CONTOUR).

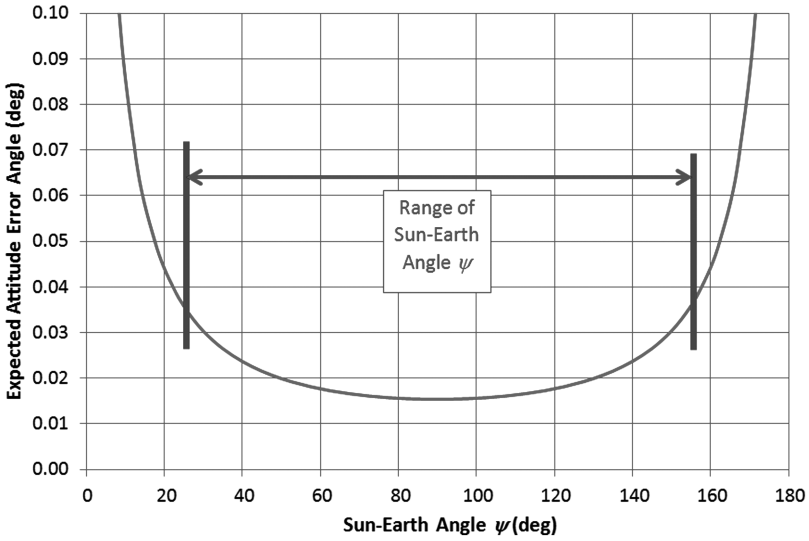

Fig. 4 Expected attitude error as function of the sun–Earth angle (MSG-2).

VIII. Conclusions

The paper establishes useful least-squares estimates and covariances for spin-axis attitude determination from sun- and Earth-sensor measurements. The use of the local reference frame defined by the instantaneous sun and Earth directions leads to a better understanding of the attitude determination error as a function of the sun–Earth angle. The results are illustrated using the actual conditions of two orbiting satellites.

References

[1] van der Ha, J. C., "Attitude Determination Covariance Analysis for Geostationary Transfer Orbits," *Journal of Guidance, Control, and Dynamics*, Vol. 9, No. 2, March–April 1986, pp. 156–163. doi:10.2514/3.20084

[2] van der Ha, J. C., Rogers, G., Dellinger, W., and Stratton, J., "CONTOUR Phasing Orbits: Attitude Determination and Control Concepts and Flight Results," *Advances in the Astronautical Sciences*, Vol. 114, Part 2, 2003, pp. 767–781.

[3] Shuster, M. D., "Efficient Algorithms for Spin-Axis Attitude Estimation," *Journal of the Astronautical Sciences*, Vol. 31, No. 2, April–June 1983, pp. 237–249.

[4] Markley, F. L., and Sedlak, J. E., "Kalman Filter for Spinning Spacecraft Attitude Estimation," *Journal of Guidance, Control, and Dynamics*, Vol. 31, No. 6, November–December 2008, pp. 1750–1760. doi:10.2514/1.35221

[5] Wertz, J. R. (ed.), *Spacecraft Attitude Determination and Control*, Springer Scientific and Business Media, New York, 1978, Part 3.

[6] van der Ha, J. C., "Progress in Satellite Attitude Determination and Control," *Journal of the Japan Society of Aeronautical and Space Sciences*, Vol. 57, No. 666, July 2009, pp. 191–198.

[7] Janssens, F. L., and van der Ha, J. C., "On the stability of Spinning Satellites," *Acta Astronautica*, Vol. 68, Nos. 7–8, April–May 2011, pp. 778–789. doi:10.1016/j.actaastro.2010.08.008

[8] van der Ha, J. C., and Janssens, F. L., "Spin-Axis Attitude Determination from Earth Chord-Angle Variations for Geostationary Satellites," *Journal of Guidance, Control, and Dynamics*, Vol. 32, No. 5, September–October 2009, pp. 1598–1608. doi:10.2514/1.40752

[9] van der Ha, J. C., "Spin-Axis Attitude Determination Using In-Flight Data," *Journal of Guidance, Control, and Dynamics*, Vol. 33, No. 3, May–June 2010, pp. 768–781. doi:10.2514/1.46811

[10] Tanygin, S., and Shuster, M. D., "Spin-Axis Attitude Estimation," *Journal of the Astronautical Sciences*, Vol. 55, No. 1, Jan.–March 2007, pp. 107–139.

[11] Crassidis, J. L., and Junkins, J. L., *Optimal Estimation of Dynamic Systems*, Chapman & Hall, Boca Raton, FL, 2004, Chap. 1.

[12] van der Ha, J. C., "Spin Axis Attitude Determination Accuracy Model in the Presence of Biases," *Journal of Guidance, Control, and Dynamics*, Vol. 29, No. 4, July–Aug. 2006, pp. 799–809. doi:10.2514/1.17745